



# Differential roles of blockade of CaV2.2-alpha2/delta1-beta1 subtype calcium channel on two models' of peripheral neuropathic pain

Chandrashekhar D. Upasani<sup>1</sup> , Abdulla K. Sherikar<sup>1,2\*</sup> 

<sup>1</sup>SNJB's SSDJ College of Pharmacy, Chandwad, Affiliated to Savitribai Phule Pune University, Pune, India.

<sup>2</sup>Department of Pharmacology, SVKM Institute of Pharmacy, Dhule, Affiliated to Dr. Babasaheb Ambedkar Technological University, Lonere, India.

## ARTICLE HISTORY

Received on: 08/01/2023  
Accepted on: 29/05/2023  
Available Online: XX

### Key words:

N-type voltage-gated calcium channel (VGCC), allodynia and hyperalgesia, antioxidants, cytokines, molecular docking.

## ABSTRACT

Although N-type voltage-gated calcium channels (VGCCs) are implicated in neuropathic pain, their biological ramifications are unknown. As a result, we investigated the neuroprotective efficacy of topiramate (TPM) and zonisamide (ZNS) against peripheral neuropathy induced by CaV2.2-alpha2/delta1-beta1 subtype of VGCC. The molecular docking analysis was conducted using a protein database to uncover the role of the human N-type VGCCs CaV2.2-alpha2/delta1-beta1 (7 VFV). Male Albino Wistar rats were treated for sciatic nerve constriction injury and a single intraperitoneal injection of streptozotocin (60 mg/kg). Following the 2-week post-neuropathy, 20 mg/kg/day intraperitoneal injections of TPM and ZNS were given. At the conclusion of each week, behavioral signs, such as allodynia and hyperalgesia, were evaluated. Following that, the sciatic nerve was extracted, the homogenate was used for biochemical analysis, and a histological study was performed. TPM and ZNS were discovered to be effective CaV2.2-alpha2/delta1-beta1 blockers via molecular docking. Total calcium and Ca<sup>2+</sup> ATPase levels in the tissues were also found to be lower. TPM and ZNS significantly reduced allodynia and hyperalgesia while also exhibiting helpful antioxidant qualities by lowering malonaldehyde and nitric oxide and raising glutathione, superoxide dismutase, and catalase levels. Furthermore, pro-inflammatory cytokines, such as tumor necrosis factor, interleukin-1, and interleukin-6, were reduced. Histopathological investigation revealed normal morphology of the sciatic nerve with no evidence of neuropathy. TPM and ZNS inhibit the CaV2.2-alpha2/delta1-beta1 in sciatic nerves and alleviate a state of neuropathy.

## HIGHLIGHTS

- CaV2.2-alpha2/delta1-beta1 subtype of N-type voltage-gated calcium channel plays a pivotal role in the development of neuropathic pain.
- CCI and STZ cause abnormal regulation in the expression of CaV2.2-alpha2/delta1-beta1.
- Topiramate and zonisamide attenuated CaV2.2-alpha2/delta1-beta1 triggering behavioral, biochemical, and histological abnormalities in the sciatic nerve.

## INTRODUCTION

Neuropathy is no longer defined by conventional dysfunction of the peripheral nervous system, but now includes damage to the somatosensory nervous system (Bouhassira, 2019). It is crucial to confirm neuropathic pain by examining changes in homeostasis balance and involvement of the somatosensory nervous system. The main contributors to neuropathic pain, according to earlier research, are diabetes, trauma, chemotherapeutic agents, alcohol, and radiation exposure (Finnerup *et al.*, 2021). Furthermore, pain researchers have made advancements in understanding chronic pain; nonetheless, controlling chronic pain is difficult due to its molecular and cellular complexity, as well as the severe impact it has on patients' normal everyday lives (Rosenberger *et al.*, 2020).

Generally, the propagation of different biological signals is well regulated by ongoing activities within the voltage-gated calcium channels (VGCC) (Zhou *et al.*,

\*Corresponding Author

Abdulla K. Sherikar; SNJB's SSDJ College of Pharmacy, Savitribai Phule Pune University, Pune, India.

E-mail: [abdullasherikar@gmail.com](mailto:abdullasherikar@gmail.com)

2020). The neurophysiological and pharmacological studies further classified these channels into L-, N-, P-, Q-, R-, and T-subtype of VGCC (Kang *et al.*, 2021). Specifically, the N-type of VGCC is crowded alongside presynaptic neuronal terminals and postsynaptic dorsal horn neurons develop synapses with afferent sensory fibers (Mao *et al.*, 2022). It is believed that these channels are involved in the propagation of peripheral painful stimuli to the central nervous system. The N-type VGCC (CaV2.2), the central point of neuronal hyperexcitation and accelerator of neurotransmitter release, plays a pivotal role in the pathogenesis of neuropathic pain (Chen *et al.*, 2021a). It is of utmost need to reform the current treatment guidelines and one step in this direction seems to block the ongoing activity of high-threshold VGCC. Moreover, despite the differing views about analgesics and opioids currently available, physicians have been reluctant to use them to control neuropathic pain. So, it is of utmost importance in both preclinical and clinical settings to shed light on the underlying cell biology and find better solutions to the problem of neuropathic pain (Rosenberger *et al.*, 2020; Teixeira-Santos *et al.*, 2020).

Patients with neuropathic conditions have abnormalities in the homeostasis of different ion channels, like voltage-gated sodium, calcium, and potassium channels, within primary afferent neurons (Finnerup *et al.*, 2021). In consequence, the ectopic activity in these neurons either causes spontaneous and stimulus-independent pain or results in an accelerated release of neurotransmitters causing overexcitation of the spinal dorsal horn. There was evidence in previous reports referring to rat brain homogenate that gabapentinoids had a greater affinity to the  $\alpha 2\delta 1$  subunit of voltage-gated  $\text{Ca}^{2+}$  channels (Chen *et al.*, 2022). Following peripheral nerve injury, the increased level of  $\alpha 2\delta 1$  subunit was observed that increases  $\text{Ca}^{2+}$  current and develops chronic pain. When the peripheral nerves are exposed to toxic free radicals, nociceptive afferent receptors become more responsive and the propagation of impulses in the dorsal root ganglia of central neurons becomes more rapid (Cui *et al.*, 2021; Patel and Dickenson, 2016). Earlier studies confirmed that proinflammatory cytokines and oxidative toxins are involved in the development of peripheral neuropathy. Cytokines are key factors that cause both activation and recruitment of immune cells in the lesioned neurons. The Schwann cells and glial cells are stimulated upon exposure to the stress of cytokines, like tumor necrosis factor— $\alpha$  (TNF- $\alpha$ ), interleukin -  $1\beta$  (IL- $1\beta$ ), and interleukin-6 (IL-6), that mediate the acute phase of hyperalgesia (Le Bars and Adam, 2002; Luo *et al.*, 2019; Naveed *et al.*, 2021).

Several anticonvulsant drugs in the newer generation, such as gabapentin and pregabalin, have been implicated as the first line of treatment against neuropathic pain caused by blood sugar problems, trauma, cancer, and alcohol consumption (Murphy *et al.*, 2020). In order to discover the exact mechanism that underlies their analgesic potential in the treatment of neuropathic pain, gabapentin-like drugs are being actively tested around the globe. Since non-opioid agents have become more familiar to the public and have a safer profile, the known and unknown use of these drugs has increased threefold in the last two decades (Micheli *et al.*, 2021).

Topiramate (TPM) and zonisamide (ZNS), both antiepileptic drugs (AEDs) are weak carbonic anhydrase inhibitors, and novel low-toxicity AEDs work as neuroprotective agents (Koshimizu *et al.*, 2020; Nazarbaghi *et al.*, 2017). TPM is a licensed drug that can be used to treat a variety of medical conditions, including simple epilepsy, complex partial epilepsy, generalized epilepsy, Lennox-Gastaut syndrome in children, and various trauma-induced neuropathic pain diseases (Pappagallo, 2003). ZNS is useful in treating various types of epilepsy, such as simple or complex focal, generalized tonic-clonic, generalized, absence, atypical, and tonic seizures (Bermejo and Anciones, 2009). TPM may exert neuroprotective effects by inhibiting voltage-gated  $\text{Na}^+$  and  $\text{Ca}^{2+}$  channels and produces antioxidant properties by elevation of superoxide dismutase (SOD), catalase (CAT) activity, and reduction of both serum and tissue nitric oxide (NO) levels in the kidney (Chong and Libretto, 2003). The neuroprotective mechanism of action of ZNS involves the inactivation of  $\text{Na}^+$  and T-type  $\text{Ca}^{2+}$  channels, inhibition of generation of reactive oxygen species, and blocking of the synthesis of NO (Biton, 2004).

As a result, useful advancements have been made in the screening techniques for different potential analgesic agents that may serve as better alternatives to existing drugs to treat neuropathic pain. It is important to uncover the exact mechanism responsible for the disease-induced chronic pain and neuropathic pain caused by somatosensory damage in order to separate the symptoms and underlying mechanisms involved in the development of these conditions. So, the current study was undertaken to reveal the possible role of CaV2.2 in the neuroprotective potential of TPM and ZNS against chronic constriction injury (CCI), and streptozotocin-induced (STZ) neuropathy.

## MATERIAL AND METHODS

### Drugs and chemicals

TPM (gift sample, Alembic Pharmaceutical Limited, Baroda, India), ZNS (gift sample, Sun Pharma, India) gabapentin and pregabalin (gift sample, MS University, Baroda, India), STZ (Sigma Aldrich, USA), and sodium pentobarbital (Abbott, India) were used. All the chemicals and reagents of standard grade used in the study were purchased from a reputed supplier.

Male rats of Wistar strain weighing 180–200 g were used for this study. These rats were purchased from Lacshmi Biofarms, Pune, India. Polycarbonate cages were used to house the rats and each cage had a group of four rats in it. The temperature of 22°C was maintained as per standard laboratory requirement for keeping the rats, 12 hours of alternation of bright and dark cycles, and palatable food and diet according to the guidelines outlined by the Committee for the Purpose of Control and Supervision of Experiments on Animals, India. Prior approval was obtained from Shriman Sureshdada Jain College of Pharmacy's Institutional Animal Ethics Committee (2017/01) to conduct this research study. With minimal pain, the rats have undergone surgery following the 1-week acclimatization interval.

The normal saline solution was used for preparing the drugs gabapentin (Li *et al.*, 2018), pregabalin (Li *et al.*, 2018), and ZNS drug (Bektas *et al.*, 2014), and TPM (Paranos *et al.*,

2013) was prepared in normal saline with one drop of 10 N HCl. The freshly prepared solution of 0.1 M citrate buffer having pH 4.5 was used for the preparation of a single-dose 60 mg/kg STZ (Lee *et al.*, 2019).

### Molecular docking studies

For the confirmation of the binding location of the ligand and its possible orientation and confirmation, molecular docking studies were carried out. The crystal architecture for human N-type VGCC CaV2.2-alpha2/delta1-beta1 (7 VFV) was made available from the data bank of protein (Research collaboratory for structural bioinformatics). The chem draw professional 16.0 software was used to sketch ligands and their 2D structure (i.e., test molecules (ZNS and TPM) and standard potent selective N-type VGCC antagonist drugs (gabapentin and pregabalin). Furthermore, the 2D structure was then converted to the 3D structure using chem draw professional 16.0 software for the optimization of molecular mechanics of ligands. Argus Lab 4.0.1 was used for the docking. The grid with dimensions  $X = 100$ ,  $Y = 100$ , and  $Z = 60 \text{ \AA}$  is assigned to cover the entire 3D active site of the alpha2/delta1-beta1 receptor. After the preformation of docking testing, the active site of proteins was then subjected to dynamic molecular docking followed by binding energy retrieval with the help of software. The Discovery Studio 2021 software was used for the visualization of the protein-ligand interaction.

### Induction of neuropathy by CCI

The sciatic nerve of the rat's left paw was operated upon using the method described by Bennett and Xie (1988). During sodium pentobarbital (45 mg/kg, i.p.) anesthesia (Kochi *et al.*, 2021), the four loose ligations with 4.0 chromic gut (Johnson & Johnson) to the sciatic nerve were given at a distance of about 1 mm between each tied knot. The incisions were sutured after surgery, and each rat was housed separately. Neuropathy was noticed after 14 days of surgery, and this is known as basal neuropathy. From the 15th day, i.e., basal, the rats were treated with an intraperitoneal injection of TPM and

ZNS each at 20 mg per kg body weight per day for the next 2 weeks as shown in (Fig. 1). In the present study, the 6 groups of rats were made each containing 10 rats ( $n = 10$ ) as mentioned below (Fig. 2).

### Induction of neuropathic pain by STZ

The 60 mg/kg intraperitoneal injection of STZ was used for the induction of diabetes (Lee *et al.*, 2019). Three days after STZ injection, the glucometer strip (Nipro Diagnostic, India) was used for the measurement of blood glucose level. The hyperglycaemic rats with 250 mg/dl or above blood glucose level were considered as an endpoint for confirmation of diabetes and these rats were included in the study protocol (Metwally *et al.*, 2018). The testing of behavioral parameters was carried out at the end of every week and after 4 weeks from the day of confirmation of diabetes, the neuropathy was confirmed. This confirmation of neuropathy was considered the baseline period. The test drugs like TPM and ZNS at 20 mg per kg body weight per day were injected intraperitoneally for a duration of 14 days as shown in (Fig. 3). After completion of the treatment schedule, the next day rats were subjected to phenobarbital-induced anesthesia to isolate the sciatic nerve for further biochemical parameter analysis.

In the present study, the five groups of rats were made each containing six rats ( $n = 06$ ) as mentioned below (Fig. 4).

### Assessment of behavioral parameters

The testing of behavioral parameters was carried out from 09.00 am to 04.00 pm and adequate care has taken to avoid a stressful situation among the rats.

### von Frey filaments-triggered mechanical allodynia

The mechanical allodynia was assessed using von Frey filaments (Aesthesio, Samitek Instruments, New Delhi). In brief, the individual rat was placed in a transparent box made from plexiglass having mesh at the bottom. The rat was allowed to acclimatize for 30 minutes before applying the von Frey filaments. In the context of pain, the sudden withdrawal of a paw or flinching was regarded as

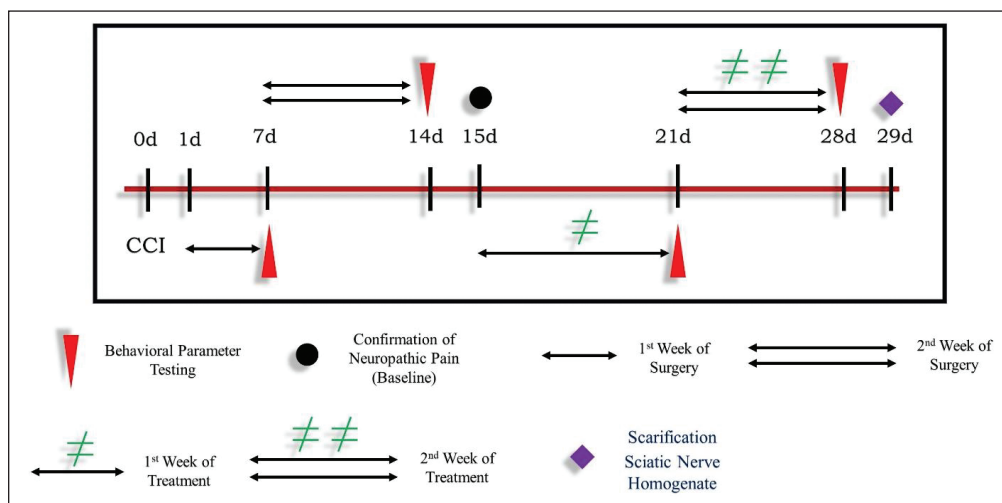


Figure 1. Development of neuropathy by CCI.

a positive response, and failure to withdraw a paw was considered a negative response. First, the filament with 2.0 g force was applied perpendicularly to the ipsilateral (left) hind paw for 3 seconds until the filament bend. As per the method described by Dixon's up-down, if the rat showed a positive response, a weaker force was applied and if the rat showed a negative response, the filament with increased force (a stronger stimulus) was applied. Each filament was applied thrice keeping a time interval of 5 minutes between each application and an average of three applications was used for further analysis. The 50% paw withdrawal threshold (PWT) was calculated and represented in grams (g) (Bennett and Xie, 1988; Chaplan *et al.*, 1994; Chen *et al.*, 2019).

#### Mechanical or static hyperalgesia by Randall-Selitto

As a sign of mechanical hyperalgesia, the paw PWT due to evoked pressure was assessed by the Randall-Selitto (Randall-Selitto Apparatus, Orchid Scientific, Nashik) method. According to this method, the applied pressure was increased at a speed of 10 g/second to the center of the ipsilateral hind paw. The moment at which the rat withdraws its hind paw or vocalizes was considered a positive response. The final pressure was recorded and represented in unit mass as gram (g). To avoid injury to the rat, the cut-off pressure was set to be 450 g, and each ipsilateral paw was tested thrice at an interval of 5 minutes between each application. The mean of three readings was then used for further statistical analysis (Levy *et al.*, 1999).

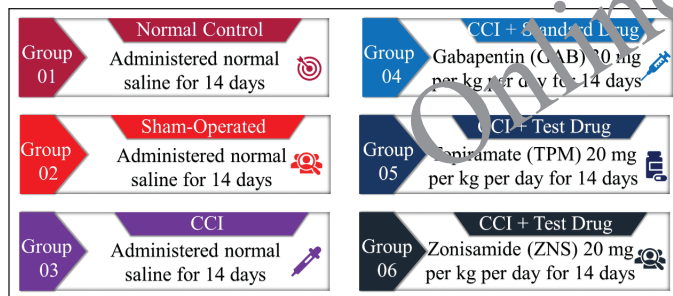


Figure 2. CCI: test drug treatment schedule.

#### Mechanical or tactile hyperalgesia by pinprick

As per the procedure described by the Bischofs, a safety pin was used to assess tactile hyperalgesia as a part of the pinprick test. In brief, the individual rat was placed in the acrylic box with a stainless sieve at the bottom. On the plantar region of the ligated hind paw, a safety pin was applied at an angle of 90° until the rat withdraws its paw. This point is considered a positive response and the minimum of 10 seconds time was used as an endpoint in order to minimize any injury to tissue. Each rat was exposed to the pin thrice at an interval of 15 minutes between each application and a mean of three readings was used for further statistical analysis (Bischofs *et al.*, 2004).

#### Cold allodynia by acetone

The paw withdrawal latency (PWL), as an index of cold allodynia, was assessed according to the method described by Lee *et al.* (2019), Yoon *et al.* (1994). As described in the method, the cotton bud with a single bubble of acetone (10 µl) was placed on the mid-plantar region of the ipsilateral hind paw, and withdrawal of the paw was considered a positive response. The 20 seconds cut-off time was set to avoid tissue damage and each paw was tested three times keeping a 15-minutes time interval between each test. The mean of three readings was then used for further calculation (Li *et al.*, 2019).

#### Assessment of oxidative stress parameters (endogenous antioxidant defense)

#### Tissue homogenization

After completion of the treatment schedule, the individual rat was sacrificed and the isolated sciatic nerve was placed in an ice-cold tris hydrochloride buffer whose pH was maintained to 7.4. With the help of a surgical chopping scalpel, the fine cross slices of tissue were prepared and placed in a chilled 0.25 M sucrose solution. The resultant solution was homogenized with 10% w/v of tris hydrochloric buffer (10 mM, pH7.4) followed by cooling centrifugation at 10,000 rpm for 15 minutes in 0°C environment. The final supernatant was used for the estimation of different parameters, like oxidative

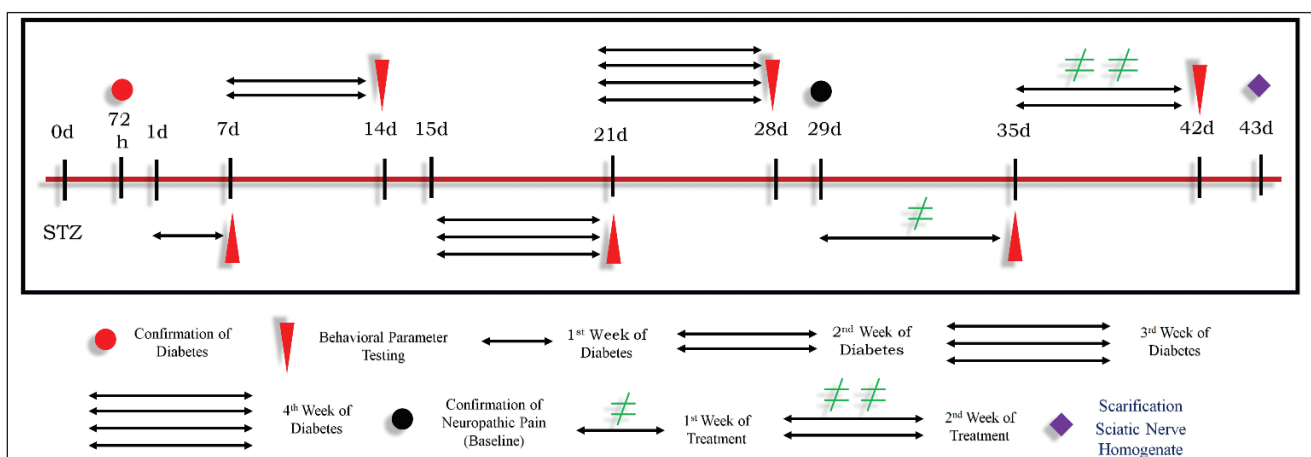


Figure 3. Induction of neuropathic pain by STZ.

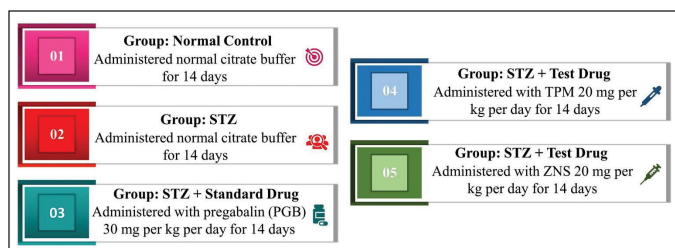


Figure 4. STZ: test drug treatment schedule.

stress, cytokines, and total calcium (Jibira *et al.*, 2020; Slater and Sawyer, 1971).

#### Estimation of lipid peroxide malonaldehyde (MDA content)

The tissue level of MDA, and the significance of lipid peroxidation were carried out as per the procedure suggested by Slater and Sawyer (1971). Briefly, the 2.0 ml of supernatant was mixed with 10% *w/v* trichloroacetic acid (TCA), and the reaction mixture was then placed in an ice bath for 15 minutes. It was followed by centrifugation to separate the formed precipitate, and the remaining clear supernatant was then mixed with freshly prepared 2.0 ml of thiobarbituric acid. Again, the resultant solution was subjected to a water-bath boiling for a period of 10 minutes followed by cooling on ice for a further 5 minutes. Cooling of the solution imparts a color, and the intensity of color was analyzed spectrophotometrically at 532 nm against a blank reagent. The different concentrations of standard MDA were then prepared and plotted on a standard graph. The MDA content in tissue homogenate was then expressed as  $\mu\text{M}$  of MDA/mg protein (Slater and Sawyer, 1971).

#### Estimation of reduced glutathione (GSH)

In this study, reduced GSH was quantitatively measured as per the procedure described by Moron *et al.* (1979). This procedure uses the principle whereby the non-proteinous thiol functional part of GSH, when reacted with dithionitrobenzene (DTNB), forms a yellow-colored complex at 412 nm. In accordance with the procedure, the precipitated material was made by mixing an equal amount of supernatant with a 20% TCA solution. After centrifuging the reaction mixture, the supernatant was separated. In the next step, 0.25 ml of the supernatant was mixed with 2 ml of DTNB, and the developed color was measured at 412 nm. The GSH was expressed as  $\mu\text{g}$  of GSH/mg of protein (Moron *et al.*, 1979).

#### Estimation of SOD

SOD neutralizes superoxide radicals and prevents adrenaline from being oxidized into its colorful by-product, adrenochrome. According to Misra and Fridovich (1972), equivalent amounts of homogenate of tissue were mixed in distilled water, then 0.25 ml cold ethanol was added and 0.15 ml chloroform was added. Following 5 minutes of mixing on a cyclo-mixer and centrifugation at 2,500 rpm, 0.5 ml of supernatant was taken, and 1.5 ml of carbonate buffer and 0.5 ml of ethylenediaminetetraacetic acid solution were added to the

reaction mixture. Following this, 0.4 ml of epinephrine was added, the optical density per minute was determined at 480 nm, and the SOD activity was measured in units per mg of protein (Misra and Fridovich, 1972).

#### Estimation of CAT

Spectrophotometric measurement of CAT activity in the sciatic nerve was performed using the method described by Aebi (1984). The basis of this method is the determination of the decomposition rate of hydrogen peroxide ( $\text{H}_2\text{O}_2$ ). To start, 1 ml of phosphate buffer (50 mmol/l; pH 7.0) was added to the supernatant. A diluted test sample of 2 ml was mixed with a solution of 1 ml of  $\text{H}_2\text{O}_2$  (30 mmol/l). The decline in absorbance was measured and represented as micromoles of  $\text{H}_2\text{O}_2$  consumed per minute per mg of protein (Murthy *et al.*, 2005).

#### Estimation of NO

The nitrite concentration was measured as a function of NO activity using the procedure described by Guevara *et al.* (1998). As stated in the procedure, 1 ml of Griess reagent was mixed with 1 ml of tissue homogenate before incubating the mixture at room temperature for 15 minutes. The absorbance was then measured spectrophotometrically at 540 nm to estimate the concentration of nitrite (Guevara *et al.*, 1998).

#### Estimation of total calcium

The Severinghaus and Ferrebee (1950) method was used to measure total calcium concentration in sciatic nerve homogenate, with minor modifications as Muthuraman and Singh (2011) suggested. Tissue homogenate was mixed with 1 ml of 4% TCA solution. The mixture was then centrifuged at 2,000 rpm for 10 minutes, and the obtained supernatant was used to measure total calcium at 556 nm (Kandhare *et al.*, 2013).

#### Determination of calcium-dependant adenosine triphosphatase ( $\text{Ca}^{2+}$ -ATPase)

A method developed by Hjertén and Pan (1983) was used to measure the  $\text{Ca}^{2+}$ -ATPase level in the sediment after tissue homogenization. In the initial trial, 0.1 ml of each Tris hydrochloride buffer (125 mM, pH 7.5), 50 mM  $\text{CaCl}_2$  solution, 10 mM adenosine triphosphate solution, and tissue homogenate were incubated for 15 minutes at 36°C. 1.0 ml of 10% *w/v* TCA solution was added afterward, and the mixture was thoroughly mixed and centrifuged. After separation, the supernatant was spectrophotometrically measured at 620 nm to determine phosphorous content. The  $\text{Ca}^{2+}$ -ATPase activity was calculated as  $\mu\text{M}$  of inorganic phosphorous liberated per mg of protein per minute (Hjertén and Pan, 1983).

#### Assessment of inflammatory markers

The tissue concentration of different inflammatory markers, like TNF- $\alpha$ , IL-1 $\beta$ , and IL-6, was determined as per the manufacturer's procedure mentioned in the mouse eBioscience Elisa kit. The 96-microtiter plate was used and absorbance was read at 450 nm. The concentrations of TNF- $\alpha$ , IL-1 $\beta$ , and IL-6 were expressed as picograms/mg of total proteins (Chen *et al.*, 2021b).

### Histopathology of the sciatic nerve

In the wake of the post-treatment schedule, the rat was sacrificed under anesthesia, and its sciatic and spinal nerves were isolated. Following that, the tissues were placed in a 10% formalin solution to maintain their normal architecture. The nerves were cut into 4 mm thick pieces for histopathology, and hematoxylin and eosin staining was performed. The neuropathological changes were observed using a light microscope on nerve sections (Singh *et al.*, 2020).

### Statistical analysis

Data were represented as mean  $\pm$  SEM. Data were analyzed with Graph Pad Prism software version 5.0. To determine the effect of treatment, results were analyzed by one-way (ANOVA) followed by *post hoc* Dunnett's test. The level of statistical difference at  $p < 0.05$  was considered as significant.

## RESULTS

### Molecular docking study of TPM and ZNS

In this context, the binding data obtained from Argus Lab revealed that ZNS has a good affinity toward alpha2/delta1-beta1 receptor with binding energy  $-9.5$  kcal/mol. While gabapentin, pregabalin, and TPM bind with receptors with binding energy  $-9.2$ ,  $-8.3$ , and  $-7.9$  kcal/mol (Table 1). Analysis of residual interaction between the blocker and target protein at the active binding site revealed that the gabapentin and pregabalin bind with CaV2.2-alpha2/delta1-beta1 receptor at two different positions by van der Waals interaction, conventional hydrogen bond, and Pi-alkyl interaction (Fig. 5). Out of nine amino acid residue which interacts with gabapentin, eight amino acids were found common with test compound (ZNS) (Table 1). ZNS bind with CaV2.2-alpha2/delta1-beta1 receptor by van der Waals interaction, Pi-Sulfur, Pi-Pi Stacked, Pi-Pi T-shape, d and Pi-alkyl interaction (Fig. 6a and b) in a similar fashion as that of standard drug gabapentin with eight common amino acid residue. These interaction patterns give a strong impression that ZNS possesses good blocking potential against CaV2.2-alpha2/delta1-beta1 receptor with gabapentin. While binding interaction pattern of TPM suggests that it might be bound to another binding pocket of CaV2.2-alpha2/delta1-beta1 receptor with respect to ZNS and TPM (Figs. 5 and 6).

### Effect of TPM and ZNS on von Frey filaments-triggered mechanical allodynia

The CCI and STZ are frequently employed and well-reported methods for the induction of neuropathic pain in rats. After performing CCI to the sciatic nerve and a single STZ intraperitoneal injection, a significant decrease in PWT was observed in all two methods of neuropathy (CCI— $2.11 \pm 0.74$  vs. Sham— $11.93 \pm 1.26$ ,  $p < 0.001$ ; STZ— $2.00 \pm 0.54$  vs. Normal— $12.18 \pm 1.03$ ,  $p < 0.001$ ). The 2 weeks treatment of gabapentin (30 mg/kg, i.p.) and pregabalin (30 mg/kg, i.p.) significantly increases the PWT as compared to CCI ( $p < 0.001$  for both weeks) and STZ-

treated rats ( $p < 0.001$  for both weeks), respectively. Like gabapentin and pregabalin, during the 2 weeks of the post-neuropathy period, the treatment with TPM (CCI and STZ-  $p < 0.01$  for both weeks) and ZNS (CCI and STZ-  $p < 0.01$  for both weeks) significantly increases the PWT as compared to sham-operated and normal rats (Fig. 7).

### Effect of TPM and ZNS on mechanical or static hyperalgesia by Randall–Selitto

Generally, mechanical or static hyperalgesia is an exaggerated painful stimulus to noxious stimuli, and to examine this phenomenon, the Randall–Selitto test apparatus was employed in the present study. In the context of neuropathy, the employed methods of neuropathy cause a reduction in PWT as an index of mechanical hyperalgesia (CCI— $75.88 \pm 8.56$  vs. Sham— $141.88 \pm 3.71$ ,  $p < 0.001$ ; STZ— $72.33 \pm 8.78$  vs. Normal— $154.2 \pm 2.49$ ,  $p < 0.001$ ). The 2 weeks treatment of gabapentin and pregabalin significantly increases the PWT as compared to CCI ( $p < 0.01$  for first week and  $p < 0.001$  for second week), and STZ-treated rats ( $p < 0.001$  for both weeks), respectively. Like gabapentin and pregabalin, during the 2 weeks of the post-neuropathy period, the treatment with TPM (CCI and STZ-  $p < 0.05$  for first week, and  $p < 0.01$  for second week) and ZNS (CCI and STZ-  $p < 0.05$  for first week, and  $p < 0.01$  for second week) significantly increases the PWT as compared to sham-operated and normal rats (Fig. 8).

### Effect of TPM and ZNS on mechanical or tactile hyperalgesia by pinprick

To investigate the CCI and STZ-triggered mechanical or tactile hyperalgesia, the pinprick test was employed and the results of the current study confirmed the development of neuropathy which was characterized by a significant reduction in the PWT (CCI— $3.30 \pm 0.74$  vs. Sham— $8.62 \pm 0.14$ ,  $p < 0.001$ ; STZ— $3.42 \pm 0.78$  vs. Normal— $8.76 \pm 0.19$ ,  $p < 0.001$ ). The post-neuropathy 2 weeks treatment of gabapentin and pregabalin significantly increases the PWT as compared to CCI ( $p < 0.01$  for first week and  $p < 0.001$  for

**Table 1.** Docking results of ligands and standard drugs against human N-type VGCC CaV2.2-alpha2/delta1-beta1 (7 VFV).

Compound ID(s)	Binding energy (kcal/mol)	Enzyme's binding site residue
Gabapentin	-9.2	240 ILE, 244 PHE, 245 TYR, 331 TRP, 332 ASN, 334 LEU, 335 TYR, 1,566 PHE, 1,569 LEU
Pregabalin	-8.3	613 LEU, 616 LEU, 617 PHE, 620 ILE, 657 PHE, 660 LEU, 700 LEU, 704 PHE, 1,401 VAL, 1,405 PHE
ZNS	-9.5	240 ILE, 244 PHE, 245 TYR, 331 TRP, 322 ASN, 335 TYR, 1,566 PHE, 1,569 LEU
TPM	-7.9	504 TYR, 1,343 LYS, 1,347 HIS, 1,349 ASP, 1,350 ASN, 1,353 TRP

Grid parameters (Argus Lab.): Spacing 0.4 Å and Grid size 100X Å, 100Y Å and 60Z Å.

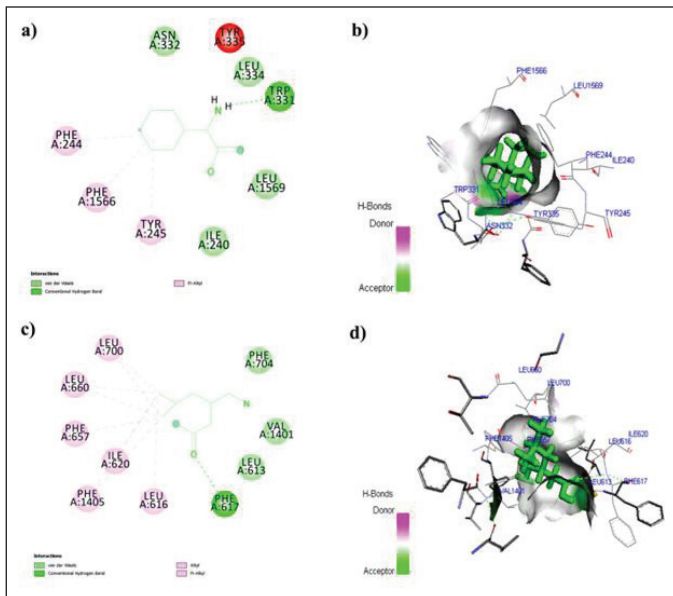


**Figure 5.** a) 2D; b) 3D: representation of the interaction of Gabapentin with human N-type VGCC CaV2.2-alpha2/delta1-beta1 (7 VFV) and c) 2D; d) 3D: representation of the interaction of Pregabalin with human N-type VGCC CaV2.2-alpha2/delta1-beta1 (7 VFV).

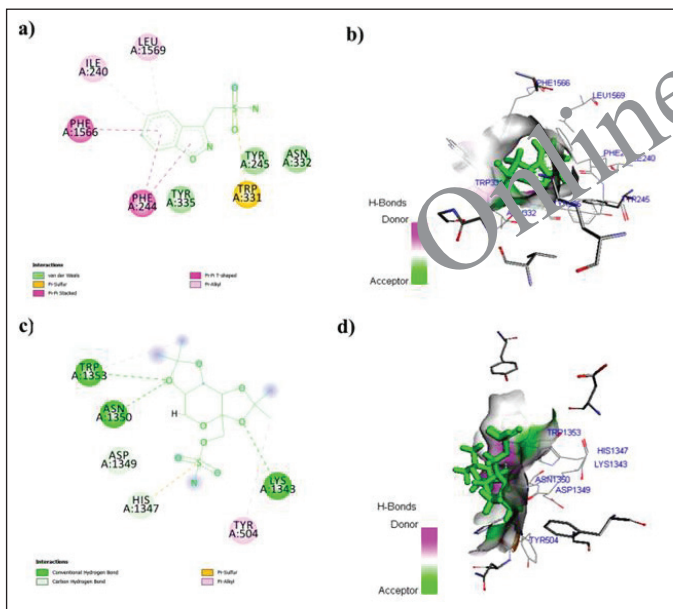


**Figure 6.** a) 2D; b) 3D: representation of the interaction of ZNS with human N-type VGCC CaV2.2-alpha2/delta1-beta1 (7 VFV) and c) 2D; d) 3D: representation of the interaction of TPM with human N-type VGCC CaV2.2-alpha2/delta1-beta1 (7 VFV).

second week), and STZ-treated rats ( $p < 0.01$  for first week and  $p < 0.001$  for second week), respectively. Like gabapentin and pregabalin, during the 2 weeks of the post-neuropathy treatment schedule, the TPM (CCI— $p < 0.01$  for first week and  $p < 0.001$  for second week; STZ— $p < 0.05$  for first week and  $p < 0.01$  for second week) and ZNS (CCI and STZ— $p < 0.05$

for first week and  $p < 0.01$  for second week) significantly increases the PWT as compared to sham-operated and normal rats (Fig. 9).

#### Effect of TPM and ZNS on cold allodynia by acetone

The sensitivity to cold stimuli was investigated by calculating the PWL triggered by acetone. The current study showed that acetone-mediated cold allodynia was significantly developed in all two methods of neuropathy characterized by a decrease in PWL (CCI— $5.27 \pm 1.79$  vs. Sham— $17.02 \pm 1.13$ ,  $p < 0.001$ ; STZ— $5.38 \pm 1.64$  vs. Normal— $17.00 \pm 0.94$ ,  $p < 0.001$ ). The daily 2 weeks post-surgery intraperitoneal injection of gabapentin (CCI— $p < 0.01$  for first week and  $p < 0.01$  for second week) and pregabalin (STZ— $p < 0.001$  for both weeks) significantly increases the PWL. Likewise, the two test drugs TPM (CCI— $p < 0.05$  for first and  $p < 0.01$  second week, and STZ— $p < 0.01$  for both weeks) and ZNS (CCI and STZ— $p < 0.05$  for both weeks) significantly increases the PWL as compared to sham-operated and normal rats (Fig. 10).

#### Effect of TPM and ZNS on total calcium

The remarkable and significant elevation in the concentration of total calcium was observed in all methods of neuropathy (CCI— $19.77 \pm 2.09$  vs. Sham— $3.41 \pm 0.88$ ,  $p < 0.001$ ; STZ— $22.16 \pm 2.56$  vs. Normal— $6.10 \pm 0.71$ ,  $p < 0.001$ ). The daily 2 weeks post-surgery intraperitoneal injection of gabapentin (CCI— $p < 0.001$ ) and pregabalin (STZ— $p < 0.001$ ) significantly decreases the level of total calcium as compared to sham-operated and normal rats, respectively. Likewise, the two test drugs TPM and ZNS (CCI and STZ— $p < 0.05$ ) significantly decrease the level of total calcium as compared to sham-operated and normal rats (Fig. 11).

#### Effect of TPM and ZNS on Ca<sup>2+</sup>-ATPases

A significant increase in Ca<sup>2+</sup>-ATPase level was observed in all methods of neuropathy (CCI— $971.90 \pm 118.80$  vs. Sham— $286.30 \pm 83.49$ ,  $p < 0.001$ ; STZ— $6,870.00 \pm 712.10$  vs. Normal— $3,120.00 \pm 490.40$ ,  $p < 0.001$ ). The gabapentin injection for 2 weeks significantly reduces the Ca<sup>2+</sup>-ATPase level in CCI-ligated whereas pregabalin in STZ-induced neuropathy ( $p < 0.001$ ). Furthermore, the TPM and ZNS injection also significantly decreases ( $p < 0.05$ ) the elevated levels of Ca<sup>2+</sup>-ATPase in all methods of neuropathy (Fig. 12).

#### Effect of TPM and ZNS on antioxidant parameters

The CCI significantly and severely disturbed the equilibrium between the reactive oxygen species (ROS) and antioxidant parameters characterized by elevated levels of MDA ( $717.60 \pm 59.33$  vs. Sham— $208.80 \pm 37.90$ ,  $p < 0.001$ ) and NO ( $13.06 \pm 1.48$  vs. Sham— $3.77 \pm 0.78$ ,  $p < 0.001$ ), and decreased GSH ( $1,617.00 \pm 149.30$  vs. Sham— $2,680.00 \pm 127.70$ ,  $p < 0.001$ ), SOD ( $2.64 \pm 0.76$  vs. Sham— $9.90 \pm 1.07$ ,  $p < 0.001$ ), and CAT ( $228.10 \pm 34.48$  vs. Sham— $616.10 \pm 38.50$ ,  $p < 0.001$ ) concentration in the homogenate of the sciatic nerve. The daily 2 weeks post-surgery intraperitoneal injection of gabapentin

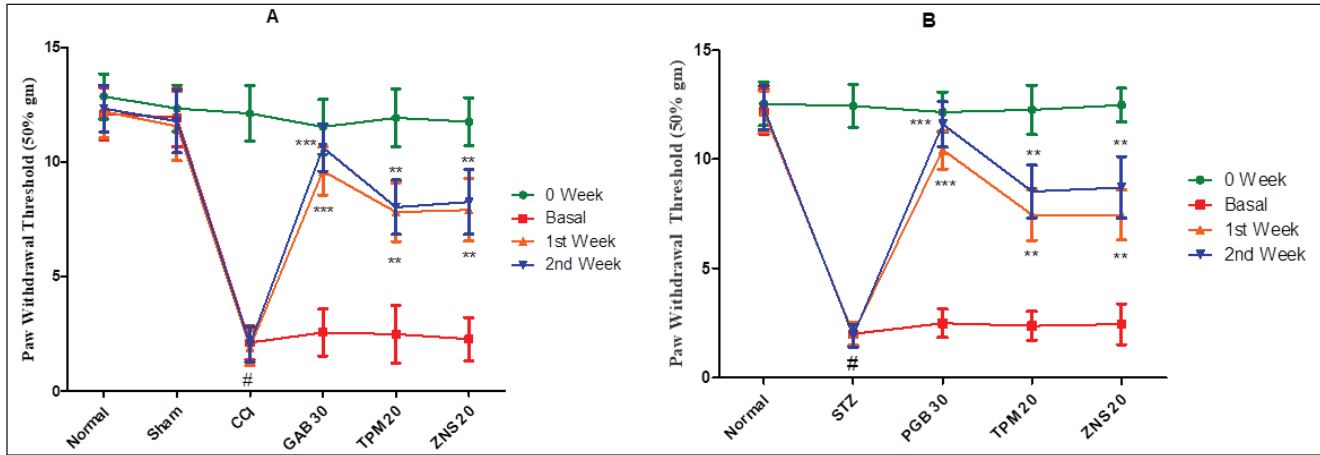


**Figure 7.** Effect of TPM and ZNS on mechanical allodynia against (A) CCI and (B) STZ. Data are expressed as mean  $\pm$  SEM and analyzed by one-way ANOVA followed by Dunnett's test (CCI— $n = 10$  and STZ— $n = 06$ ). # $p < 0.001$  against sham-operated and normal rats when compared with unpaired student  $t$ -test); \* $p < 0.05$ , \*\* $p < 0.01$  and \*\*\* $p < 0.001$  against CCI, and STZ rats.

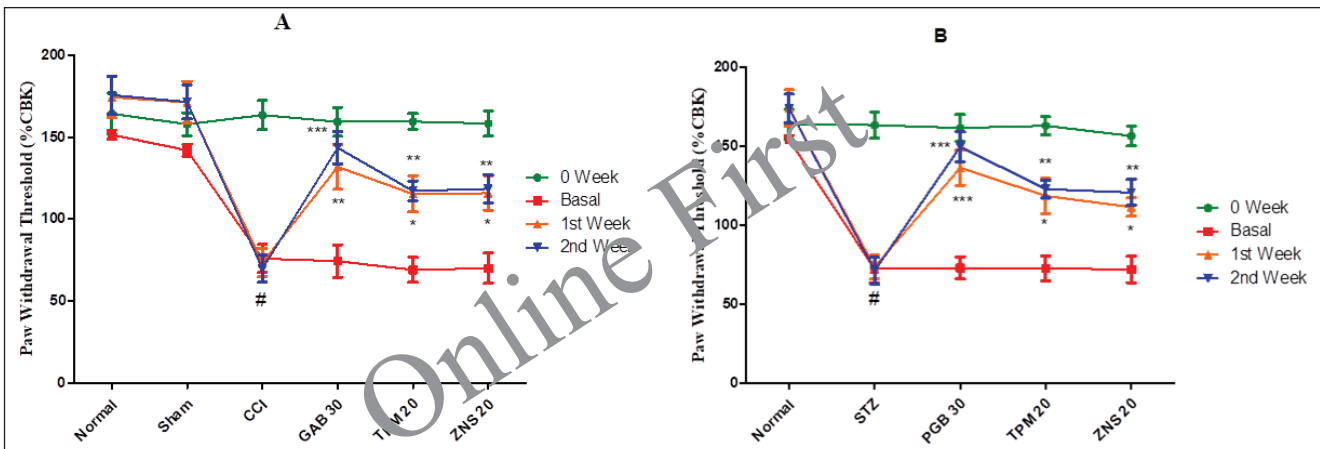


**Figure 8.** Effect of TPM and ZNS on mechanical or static hyperalgesia against (A) CCI, and (B) STZ. Data are expressed as mean  $\pm$  SEM and analyzed by one-way ANOVA followed by Dunnett's test (CCI— $n = 10$  and STZ— $n = 06$ ). # $p < 0.001$  against sham-operated and normal rats when compared with unpaired student  $t$ -test); \* $p < 0.05$ , \*\* $p < 0.01$  and \*\*\* $p < 0.001$  against CCI and STZ rats.

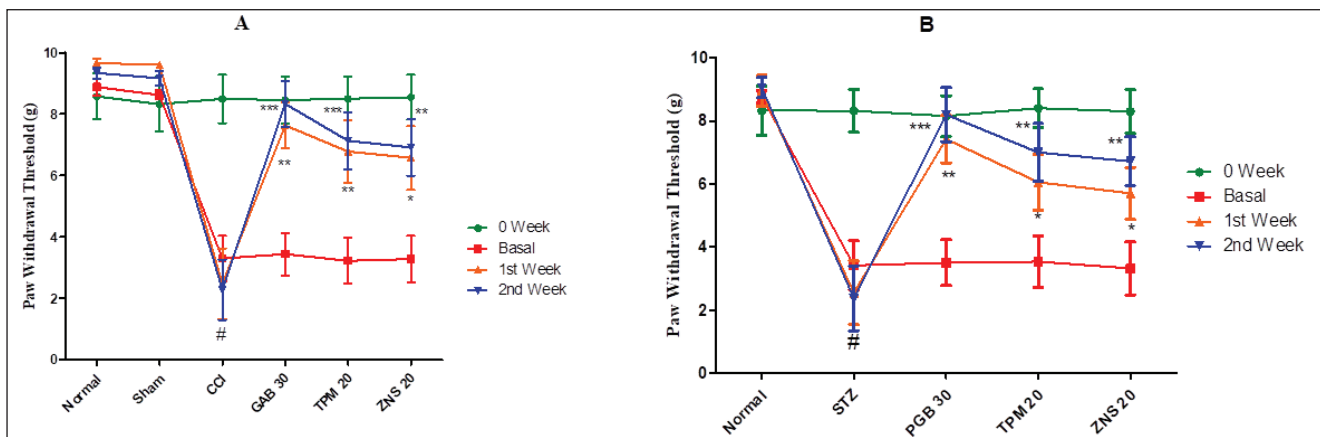


**Figure 9.** Effect of TPM and ZNS on mechanical or tactile hyperalgesia against (A) CCI, and (B) STZ. Data are expressed as mean  $\pm$  SEM and analyzed by one-way ANOVA followed by Dunnett's test (CCI— $n = 10$  and STZ— $n = 06$ ). # $p < 0.001$  against sham operated and normal rats when compared with unpaired student  $t$ -test); \* $p < 0.05$ , \*\* $p < 0.01$  and \*\*\* $p < 0.001$  against CCI and STZ rats.

significantly attenuated the development of oxidative damage highlighted as decreased levels of MDA and NO, and elevated levels of GSH, SOD, and CAT ( $p < 0.001$ ) as compared to the CCI-ligated rats. Likewise, the two test drugs TPM and ZNS injection for 2 weeks of post-surgery also significantly attenuated the development of oxidative damage highlighted as decreased levels of MDA and NO, and elevated level of GSH, SOD, and CAT ( $p < 0.05$ ) as compared to the CCI-ligated rats. Additionally, ZNS showed remarkable potent inhibitory effects on the level of NO ( $p < 0.01$ ) as compared to CCI-ligated rats (Fig. 13).

In the line of STZ-triggered neuropathy, the current study confirmed the development of neuropathy and was associated with remarkable changes in the level of ROS. The present study showed the elevated level of MDA ( $698.70 \pm 51.93$  vs. Normal— $285.40 \pm 40.05$ ,  $p < 0.001$ ) and NO ( $11.38 \pm 0.93$  vs. Normal— $2.56 \pm 0.48$ ,  $p < 0.001$ ), and decreased concentration of scavengers of ROS like GSH ( $1,600.00 \pm 181.50$  vs. Normal— $2,888.00 \pm 195.70$ ,  $p < 0.001$ ), SOD ( $2.88 \pm 0.86$  vs. Normal— $12.60 \pm 1.41$ ,  $p < 0.001$ ), and CAT ( $214.00 \pm 16.04$  vs. Normal— $583.20 \pm 41.56$ ,  $p < 0.001$ ). The daily 2 weeks post-surgery intraperitoneal injection of pregabalin significantly attenuated the development of oxidative damage highlighted as decreased levels of MDA and NO, and elevated levels of GSH, SOD, and CAT ( $p < 0.001$ ) as compared to the STZ-treated rats. Likewise, the two test drugs TPM and ZNS injection for 2 weeks of post-surgery also significantly attenuated the development of oxidative damage highlighted as decreased levels of MDA and NO, and elevated levels of GSH, SOD, and CAT ( $p < 0.05$ ) as compared to the STZ treated rats. Additionally, ZNS showed remarkable effects on levels of SOD and NO ( $p < 0.01$ ) as compared to STZ-treated rats (Fig. 14).

#### Effect of TPM and ZNS on inflammatory markers

As a consequence of inflammation, different biological markers, like TNF- $\alpha$ , IL-1 $\beta$ , and IL-6, were estimated in the homogenates of the sciatic nerve. As previously reported, the present study also confirmed the CCI-triggered neuropathic inflammatory situation characterized by elevated levels of TNF- $\alpha$  ( $2,212.00 \pm 212.60$  vs. Sham— $733.80 \pm 241.40$ ,  $p < 0.001$ ), IL-1 $\beta$  ( $1,543.00 \pm 187.50$  vs. Sham— $386.20 \pm 122.50$ ,

$p < 0.001$ ), and IL-6 ( $1,667.00 \pm 190.40$  vs. Sham— $367.30 \pm 131.40$ ,  $p < 0.001$ ). The post-surgery treatment of gabapentin significantly attenuated the inflammatory condition by lowering the levels of TNF- $\alpha$ , IL-1 $\beta$ , and IL-6 ( $p < 0.001$ ) as compared to CCI-ligated rats. Similarly, TPM and ZNS injection also significantly decreases ( $p < 0.05$ ) the elevated levels of biological markers of inflammation as compared to CCI-ligated rats as shown in (Fig. 15).

To investigate STZ-induced neuropathy, we have estimated the concentration of pro-inflammatory markers in the homogenate of the sciatic nerve. According to the outcome of the present study, it was found that a single dose of STZ develops painful neuropathy characterized by significant elevation of levels of TNF- $\alpha$  ( $2,324.00 \pm 207.00$  vs. Normal— $770.00 \pm 205.40$ ,  $p < 0.001$ ), IL-1 $\beta$  ( $1,599.00 \pm 193.60$  vs. Normal— $384.80 \pm 131.80$ ,  $p < 0.001$ ), and IL-6 ( $1,748.00 \pm 192.60$  vs. Normal— $373.70 \pm 136.90$ ,  $p < 0.001$ ) as compared to normal rats. Following 2 weeks treatment with pregabalin, the levels of pro-inflammatory cytokines ( $p < 0.001$ ) were found to be declined significantly as compared to the STZ-treated rats. Likewise, the injection of TPM and ZNS also significantly decreases ( $p < 0.05$ ) the elevated levels of pro-inflammatory cytokines as compared to STZ-treated rats (Fig. 16).

#### Effect of TPM and ZNS on blood glucose

To investigate STZ-induced neuropathy, we have estimated the concentration of sugar in the blood. According to the outcome of the present study, it was found that a single dose of STZ develops painful neuropathy characterized by significant elevation of blood glucose level ( $322.50 \pm 21.90$  vs. Normal— $124.20 \pm 18.55$ ,  $p < 0.001$ ) as compared to normal rats. Following 2 weeks treatment of pregabalin, TPM and ZNS did not significantly reduce the blood glucose level (Fig. 17)

#### Effect of TPM and ZNS on histopathology of the sciatic nerve

To investigate the morphological changes after CCI and STZ-induced neuropathy, a histopathological examination was carried out in the sections of the sciatic nerve. In line with

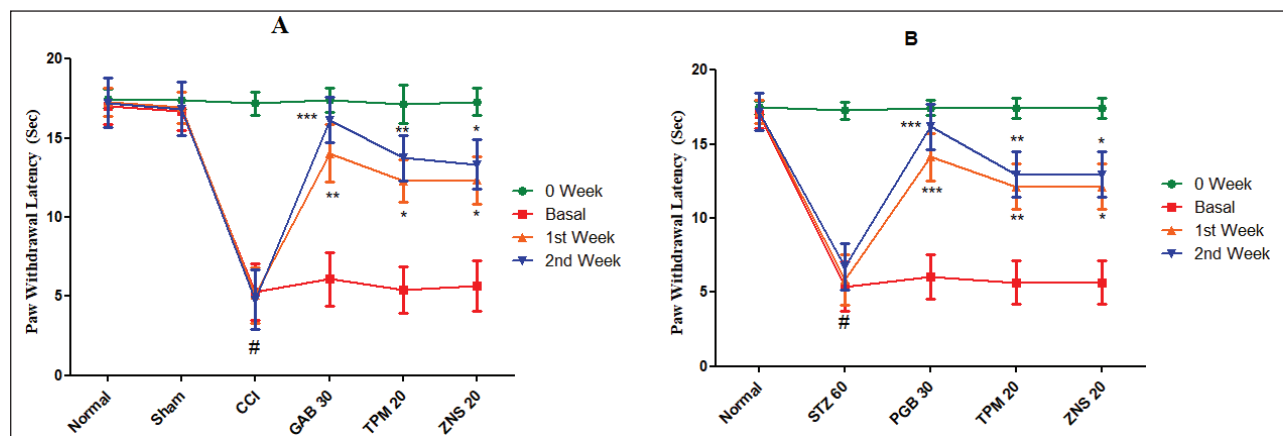


**Figure 10.** Effect of TPM and ZNS on cold allodynia against (A) CCI, and (B) STZ. Data are expressed as mean  $\pm$  SEM and analyzed by one-way ANOVA followed by Dunnett's test (CCI— $n = 10$  and STZ— $n = 06$ ). # $p < 0.001$  against sham-operated and normal rats when compared with unpaired student 't'-test); \* $p < 0.05$ , \*\* $p < 0.01$  and \*\*\* $p < 0.001$  against CCI and STZ rats.

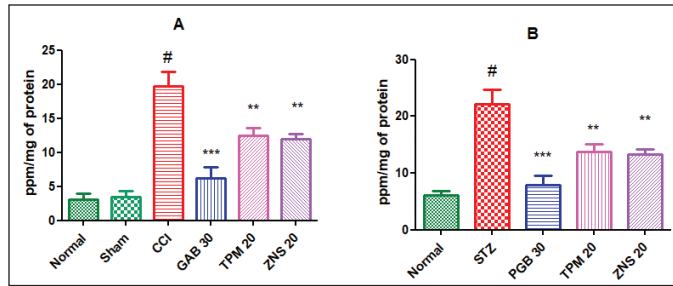


**Figure 11.** Effect of TPM and ZNS on total calcium against (A) CCI (GAB— $6.230 \pm 1.60$ , TPM— $12.42 \pm 1.18$ , ZNS— $11.92 \pm 0.73$ ), and (B) STZ (PGB— $7.940 \pm 1.57$ , TPM— $13.82 \pm 1.23$ , ZNS— $13.34 \pm 0.84$ ). Data are expressed as mean  $\pm$  SEM and analyzed by one-way ANOVA followed by Dunnett's test (CCI— $n = 10$  and STZ— $n = 06$ ). <sup>#</sup> $p < 0.001$  against sham-operated and normal rats when compared with unpaired student 't'-test); <sup>\*</sup> $p < 0.05$ , and <sup>\*\*\*</sup> $p < 0.001$  against CCI and STZ rats.

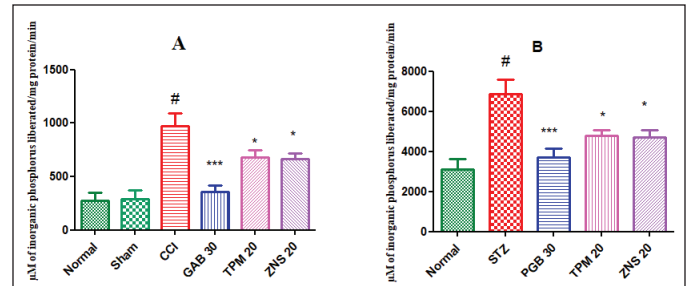


**Figure 12.** Effect of TPM and ZNS on  $\text{Ca}^{2+}$ -ATPases against (A) CCI (GAB— $355.90 \pm 62.41$ , TPM— $679.4 \pm 70.14$ , ZNS— $665.9 \pm 50.58$ ), and (B) STZ (PGB— $3,703.00 \pm 456.10$ , TPM— $4,786.00 \pm 284.7$ , ZNS— $4,709.00 \pm 349.60$ ). Data are expressed as mean  $\pm$  SEM and analyzed by one-way ANOVA followed by Dunnett's test (CCI— $n = 10$  and STZ— $n = 06$ ). <sup>#</sup> $p < 0.001$  against sham-operated and normal rats when compared with unpaired student 't'-test); <sup>\*</sup> $p < 0.05$ , <sup>\*\*</sup> $p < 0.01$  and <sup>\*\*\*</sup> $p < 0.001$  against CCI and STZ rats.

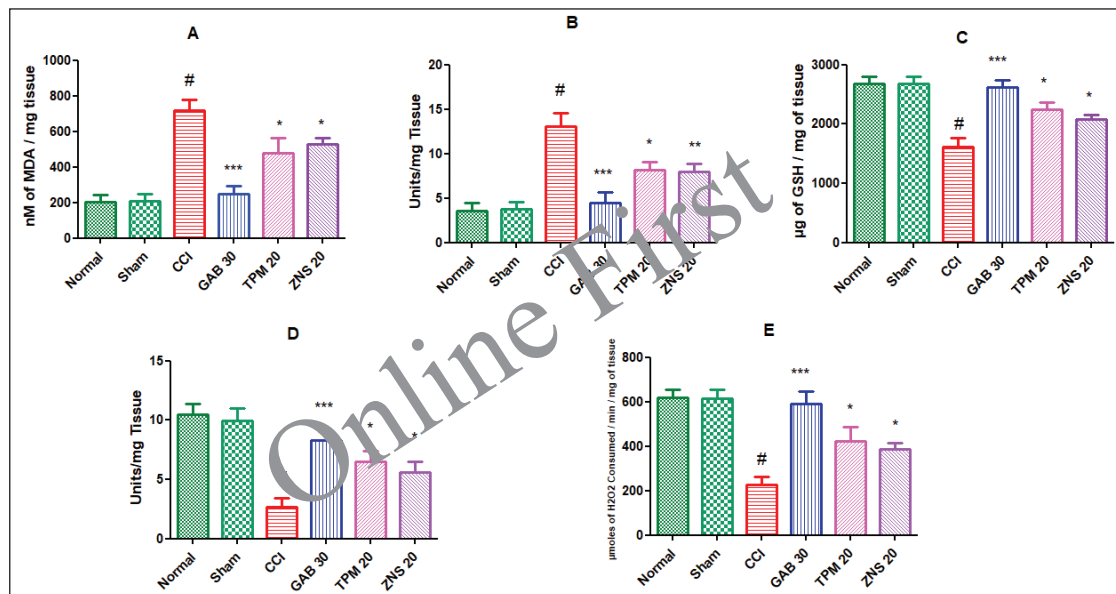


**Figure 13.** Effect of TPM and ZNS on oxidative stress against CCI. A. MDA (GAB— $247.60 \pm 46.29$ , TPM— $480.40 \pm 83.82$ , ZNS— $529.00 \pm 36.40$ ); B. NO (GAB— $4.50 \pm 1.12$ , TPM— $8.18 \pm 0.84$ , ZNS— $7.95 \pm 0.86$ ); C. GSH (GAB— $2,623.00 \pm 115.20$ , TPM— $2,239.00 \pm 123.20$ , ZNS— $2,079.00 \pm 82.40$ ); D. SOD (GAB— $8.30 \pm 0.75$ , TPM— $6.50 \pm 0.93$ , ZNS— $5.62 \pm 0.85$ ); and E. CAT (GAB— $590.70 \pm 55.64$ , TPM— $423.10 \pm 65.06$ , ZNS— $380.20 \pm 31.05$ ). Data are expressed as mean  $\pm$  SEM and analyzed by one-way ANOVA followed by Dunnett's test (CCI— $n = 10$ ). <sup>#</sup> $p < 0.001$  against sham-operated and normal rats when compared with unpaired student 't'-test); <sup>\*</sup> $p < 0.05$ , <sup>\*\*</sup> $p < 0.01$  and <sup>\*\*\*</sup> $p < 0.001$  against CCI rats.

previous reports, the CCI and STZ cause severe morphological abnormalities in the sciatic nerve section which was characterized as swelling, degeneration, and necrosis of myelin sheath along with modulation in the underlined vascular tissues. There were no changes observed in normal and sham-operated groups in both methods. The post-surgery 2 weeks intraperitoneal injection of TPM and ZNS significantly attenuated both CCI and STZ-induced sciatic nerve damage (Figs. 18 and 19), and Tables 2 and 3, respectively.

## DISCUSSION

With the advancement of the computer-based docking method in the context of drug development, and basic research,

molecular docking involves the target protein and ligand binding approach to identify a target protein's function in various disease states (Stanzione *et al.*, 2021). Since N-type VGCC  $\text{CaV}2.2\text{-}\alpha2/\delta1\text{-}\beta1$  (7 VFV) is involved in the pathogenesis of neuropathic pain (Chen *et al.*, 2022), we explored the molecular docking work to uncover the blocking property of AEDs, like TPM and ZNS, against  $\text{CaV}2.2\text{-}\alpha2/\delta1\text{-}\beta1$  (7 VFV) as such studies were not previously conducted. In light of this, we examined the *in vivo* effectiveness of these agents against  $\text{CaV}2.2\text{-}\alpha2/\delta1\text{-}\beta1$  (7 VFV) as well as their analgesic, anti-inflammatory, and NO blocking properties under different neuropathy methods, such as CCI and STZ, in male rats.

After performing *in silico* molecular docking studies, ZNS and TPM were found to block CaV2.2-alpha2/delta1-beta1 (7 VFV). Compared to gabapentin and pregabalin, ZNS binds and blocks CaV2.2-alpha2/delta1-beta1 receptors at comparable sites, whereas TPM might bind to another pocket. In summary, the results of the molecular docking study suggest that CaV2.2-alpha2/delta1-beta1 (7 VFV) is crucial to the pathogenesis of neuropathic pain, while TPM and ZNS may be neuroprotective in neuropathy caused by CCI and STZ.

It is well acknowledged that Ca<sup>2+</sup> signaling controls how excitable and non-excitable cells maintain homeostasis (Hilaire *et al.*, 2005). The coordinated movement of Ca<sup>2+</sup> ions across the cell membrane controls a variety of physiological processes, including the contraction of muscles and the release of neurotransmitters (Verkhatsky *et al.*, 2020). It is generally known that an increase in Ca<sup>2+</sup> concentration leads to oxidative stress, changes the concentration of several biochemicals, and seriously harms axon architecture (Malko and Jiang, 2020). Ca<sup>2+</sup> ATP activity in the sarco-endoplasmic reticulum disappears when Ca<sup>2+</sup> signaling control is lost, which is followed by a reduction in the amount of Ca<sup>2+</sup> that can be stored in the endoplasmic reticulum (Yang *et al.*, 2019). Studies on status epilepsy (Rajakulendran and Hanna, 2016) and neuropathic pain brought on by spinal nerve ligation (SNL) (Liu *et al.*, 2019a) point to the damaged neurons' dysregulated resting Ca<sup>2+</sup> signaling. The main finding of electrophysiological and behavioral research on various forms of inflammation suggested that calcium plays a role in the emergence of painful impulses across spinal cord neurons

(Aurilio *et al.*, 2008). Antinociceptive drugs inhibited the formation of painful sensations across the spinal cord neurons by inhibiting VGCC, and the calcium influx also caused the integration and propagation of pain impulses (Palhares *et al.*, 2017). In a similar vein, we noted increased total calcium concentration and Ca<sup>2+</sup>-ATPase activity in the sciatic nerve homogenate after CCI and STZ. As with gabapentin and pregabalin, the post-neuropathy therapy with TPM and ZNS considerably lowers the Ca<sup>2+</sup> concentration and inhibits the Ca<sup>2+</sup>-ATPase activity inside the damaged neurons.

The release of excitatory transmitters by exocytosis is triggered by the peripheral neuronal injury, which also increases electrical activity in the primary afferent nerve fibers beneath. The transmitter then stimulates the glutamate, substance P, and calcitonin gene-related peptide receptors, which results in an increase in the production of nerve impulses across the spinal cord neurons (Lee *et al.*, 2012). Additionally, it was shown that the nerve terminals that are essential for the release of the transmitters have an increased population of N-type VGCC (Liu *et al.*, 2016). Collectively, these findings imply that the continuing activity of the N-type VGCC promotes the hyper excitation of underlying neurons and facilitates neurotransmission during the persistent phase of neuropathic pain (Yang *et al.*, 2018). Numerous peripheral neuropathy-related animal models showed that the dorsal root ganglion and spinal dorsal horn neurons contained higher levels of the protein  $\alpha 2\delta 1$  which act as the pain-triggering center. Because they are effective at treating pain, medicines in the gabapentinoid class have positive analgesic effects after

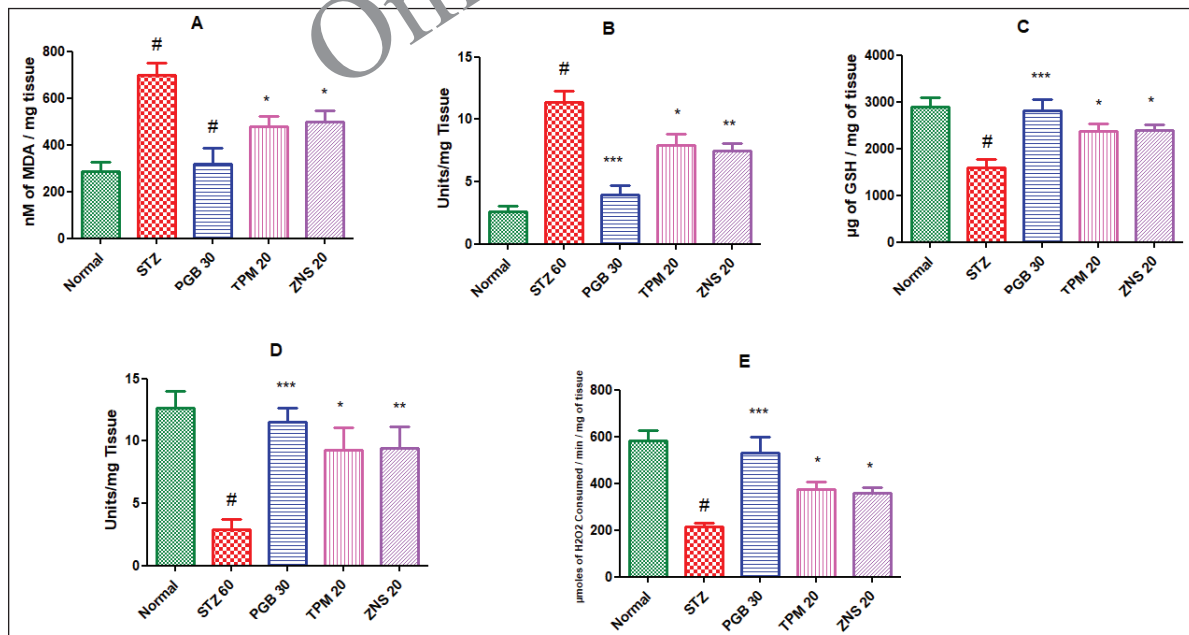


**Figure 14.** Effect of TPM and ZNS on oxidative stress against STZ. A. MDA (PGB—317.40 ± 69.37, TPM—478.90 ± 43.98, ZNS—498.90 ± 46.13); B. NO (PGB—3.91 ± 0.77, TPM—7.95 ± 0.84, ZNS—7.47 ± 0.64); C. GSH (PGB—2,822.00 ± 222.30, TPM—2,372.00 ± 169.30, ZNS—2,388.00 ± 121.00); D. SOD (PGB—11.50 ± 1.12, TPM—9.30 ± 1.74, ZNS—9.43 ± 1.75); and E. CAT (PGB—528.70 ± 70.55, TPM—374.50 ± 31.54, ZNS—356.80 ± 25.80). Data are expressed as mean ± SEM and analyzed by one-way ANOVA followed by Dunnett's test (STZ—*n* = 06). <sup>#</sup>*p* < 0.001 against sham-operated and normal rats when compared with unpaired student '*t*'-test; <sup>\*</sup>*p* < 0.05, <sup>\*\*</sup>*p* < 0.01 and <sup>\*\*\*</sup>*p* < 0.001 against STZ rats.

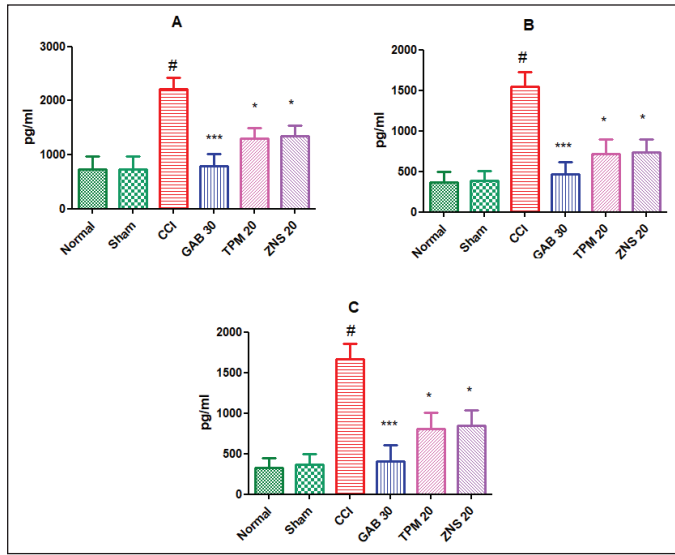


**Figure 15.** Effect of TPM and ZNS on inflammatory markers against CCI. A. TNF- $\alpha$  (GAB—785.7  $\pm$  223.00, TPM—1,302.00  $\pm$  196.40, ZNS—1,343.00  $\pm$  197.20); B. IL-1 $\beta$  (GAB—468.7  $\pm$  147.30, TPM—719.3  $\pm$  175.80, ZNS—731.7  $\pm$  161.70); C. IL-6 (GAB—404.7  $\pm$  201.90, TPM—804.5  $\pm$  199.30, ZNS—841.7  $\pm$  197.70). Data are expressed as mean  $\pm$  SEM and analyzed by one-way ANOVA followed by Dunnett’s test (CCI— $n$  = 10). # $p$  < 0.001 against sham-operated and normal rats when compared with unpaired student ‘ $t$ ’-test; \* $p$  < 0.05, and \*\*\* $p$  < 0.001 against SNL rats.

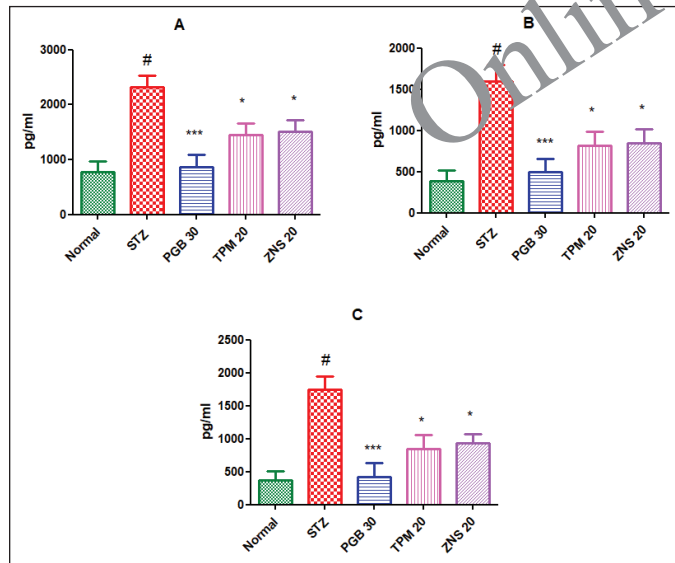


**Figure 16.** Effect of TPM and ZNS on inflammatory markers against STZ. A. TNF- $\alpha$  (PGB—496.5  $\pm$  155.30, TPM—819.0  $\pm$  170.30, ZNS—1,504.00  $\pm$  221.50); B. IL-1 $\beta$  (PGB—468.7  $\pm$  147.30, TPM—719.3  $\pm$  175.80, ZNS—847.1  $\pm$  169.60); C. IL-6 (PGB—424.3  $\pm$  204.60, TPM—847.7  $\pm$  210.10, ZNS—933.1  $\pm$  134.90). Data are expressed as mean  $\pm$  SEM and analyzed by one-way ANOVA followed by Dunnett’s test (STZ— $n$  = 06). # $p$  < 0.001 against sham-operated and normal rats when compared with unpaired student ‘ $t$ ’-test; \* $p$  < 0.05, and \*\*\* $p$  < 0.001 against SNL rats.

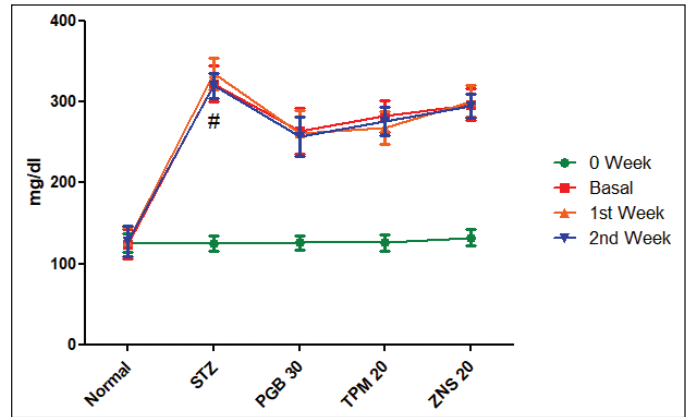


**Figure 17.** Effect of TPM and ZNS on blood glucose level against STZ (first Week = PGB—261.70  $\pm$  28.57, TPM—268.30  $\pm$  20.07, ZNS—300.80  $\pm$  19.21; second Week = PGB—257.50  $\pm$  23.94, TPM—275.80  $\pm$  17.24, ZNS—295.00  $\pm$  14.66 Data are expressed as mean  $\pm$  SEM and analyzed by one-way ANOVA followed by Dunnett’s test (STZ— $n$  = 06).

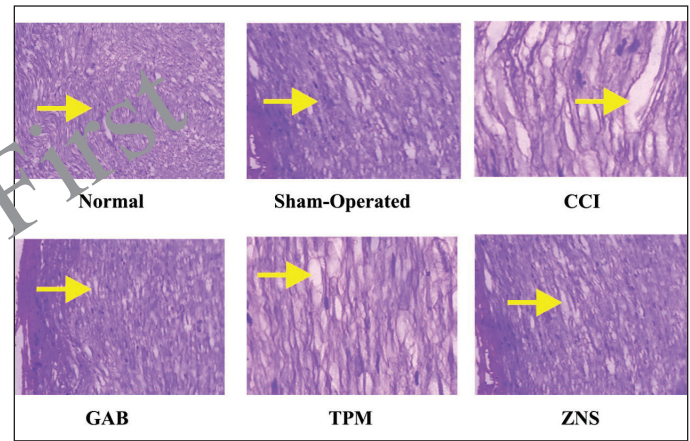


**Figure 18.** Histopathological changes observed in sciatic nerve after CCI-induced neuropathy.

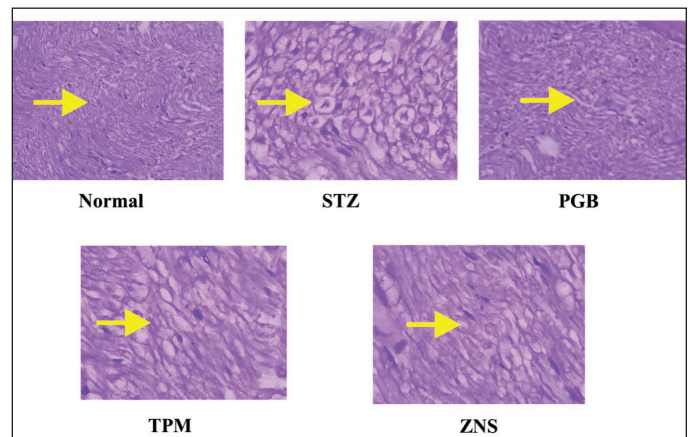


**Figure 19.** Histopathological changes observed in sciatic nerve after STZ-induced neuropathy.

**Table 2.** Histopathological changes observed in sciatic nerve after CCI-induced neuropathy.

Groups	Swelling in sheath	Degeneration	Necrotic changes	Vascular changes
Normal	-	-	-	-
Sham-operated	+	-	-	+
CCI	+++	+++	+++	+++
GAB 30	+	+	+	++
TPM 20	++	+	++	++
ZNS 20	++	+	+	++

(+++ Severe; ++Moderate; +Mild; -Nil).

**Table 3.** Histopathological changes observed in sciatic nerve after STZ-induced neuropathy.

Groups	Swelling in sheath	Degeneration	Necrotic changes	Vascular changes
Normal	-	-	-	-
STZ	+++	+++	+++	+++
PGB 30	+	+	+	++
TPM 20	+	+	++	++
ZNS 20	+	+	+	++

(+++ Severe; ++Moderate; +Mild; -Nil).

binding to the  $\alpha\delta 1$  protein (Baba *et al.*, 2020). As a result, we used the CCI and STZ models of neuropathy in the current investigation. The results of these studies demonstrated the onset of neuropathy, which was underlined by the behavioral signs of allodynia and hyperalgesia. TPM and ZNS intraperitoneally at a dose of 20 mg/kg/day after 2 weeks of post-neuropathy treatment significantly delayed the onset of mechanical and cold allodynia against von Frey filaments and acetone tests. In rats with CCI and STZ-induced neuropathy, we discovered that TPM and ZNS administration significantly increased the von Frey filament-triggered PWT and acetone-triggered PWL, indicating that these drugs had antiallodynic effects. We used the pinprick test for the generation of tactile stimuli and the Randall–Selitto apparatus for the creation of static stimuli to validate the antihyperalgesic effects of TPM and ZNS. We found that TPM and ZNS post-surgery dramatically raise the threshold value for paw withdrawal in opposition to CCI and STZ treatments of neuropathy. The results of the current study taken together point to the potential analgesic effects of TPM and ZNS against the CCI and STZ models of neuropathy.

Neurodegenerative illnesses, inflammation, ischemia, and mechanical damage have negative effects on VGCC and enhance the formation of ROS, apoptosis, and  $Ca^{2+}$  influx. The overproduction of ROS results in an increased rate of  $Ca^{2+}$  influx in the context of traumatic damage and neuropathic pain. Due to immune cell infiltration, increased ROS transport, and the accumulation of oxidative to nitrosative load surrounding the lesioned area of neurons, nerve damage is the focal site of oxidative stress (Zhang *et al.*, 2022). We also assessed the

level of several oxidative stress indicators, such as MDA, NO, GSH, SOD, and CAT, in the homogenate of the sciatic nerve following CCI and STZ in order to study the molecular process involved in the development of neuropathy. The current study supported prior results by confirming the emergence of oxidative stress conditions as seen by increased MDA and NO levels and decreased GSH, SOD, and CAT levels following CCI and STZ. We measured the amount of MDA to demonstrate the beneficial effects on lipid peroxidation, and it was shown that TPM and ZNS post-surgery therapy considerably reduced lipid peroxidation in a manner comparable to that of gabapentin and pregabalin. Typically, neuropathic pain occurs when the antioxidant process fails to keep the concentration of damaging oxidative radicals below the hazardous level (Chen *et al.*, 2021b). Surgery-induced stress causes the mitochondria to go through oxidative phosphorylation, start the production of superoxide radical, convert it to  $H_2O_2$  under the control of SOD, and create the extremely reactive hydroxyl radical (Ilari *et al.*, 2020). Therefore, we looked at the concentration of endogenous antioxidants, such as GSH, SOD, and CAT, to identify the potential mechanism involved in the antioxidant mechanism of TPM and ZNS. Our study's results demonstrated that these substances had antioxidant potential since they considerably raised GSH, SOD, and CAT concentrations to levels comparable to those of common medications like gabapentin and pregabalin. Additionally, enzymatic byproducts like SOD and NO are further transformed into reactive peroxy radicals, raising the cytoplasmic calcium concentration. The ectopic discharges into the spinal cord were caused by an outflow of inputs from lesioned primary afferent neurons, which accelerated mitochondrial respiration and increased levels of intracellular calcium and ROS production. We then looked at the concentration of NO in the sciatic nerve homogenates in order to address the NO level. Since TPM and ZNS considerably reduced the concentration of NO as that of gabapentin and pregabalin, the results of the current experiment demonstrated the favorable antioxidant effects of these drugs.

The damage to the nerve often results in cytokine-induced activation of the immune system that increases the level of pro-inflammatory cytokines and facilitated neuropathic pain. Both the preclinical and clinical studies about neuropathic pain revealed the overexpression of pro-inflammatory cytokines, like TNF- $\alpha$  (Czeschik *et al.*, 2008), IL-1 $\beta$  (Noh *et al.*, 2019), and IL-6 (Liu *et al.*, 2019b), at the site of injury. In the context of neuropathic pain, cytokine-like TNF- $\alpha$ , and IL-1 $\beta$  not only activate N type of calcium channels but also originate the evoked pain signals through these channels (Czeschik *et al.*, 2008). Peripheral nerve injury upregulates N-type calcium channels in the soma of uninjured dorsal root ganglia (DRG) neurons by over-production of IL-1 $\beta$  (Noh *et al.*, 2019). Through an increase in neuronal excitability, the overexpression of N-type calcium channels in the soma of DRG neurons may cause neuropathic pain (Czeschik *et al.*, 2008). As a result of our increasing curiosity regarding how TNF- $\alpha$ , IL-1 $\beta$ , and IL-6 regulate the continuing activity of N-type calcium channels, we measured the levels of these cytokines in the sciatic nerve homogenate after CCI and STZ. In our case, it was shown that raised levels of

TNF- $\alpha$ , IL-1 $\beta$ , and IL-6 were present following the onset of the neuropathy. The therapy with TPM and ZNS dramatically reduced the elevated concentration of these cytokines, indicating a possible anti-inflammatory effect. There was no significant effect was observed on blood glucose level after treatment with pregabalin, TPM and ZNS against STZ-induced neuropathy.

The histopathological study after CCI and STZ-induced neuropathy abnormally disturb the normal architecture of the sciatic nerve and its morphological architecture is highlighted as swelling, degeneration, and necrosis of myelin sheath and Wallerian degeneration (Singh *et al.*, 2020). Histopathological examination showed the normal morphology of the sciatic nerve without remarkable signs of neuropathy.

In conclusion, finding a better remedy against neuropathy with minimal side effects has become a challenging task. At present, multiple treatment approaches are being focused at the molecular and cellular level aiming to find a better and potential alternative remedy to current treatment guidelines. To continue this approach, the present work was undertaken to reveal the neuroprotective efficiency of TPM and ZNS against different methods of induced neuropathy like CCI and STZ. The results of the present investigation showed that TPM and ZNS exhibit potential analgesic, anti-inflammatory, and antioxidant actions by inhibiting CaV2.2- $\alpha$ 2/ $\delta$ 1- $\beta$ 1 in sciatic nerves and ameliorate a state of neuropathy. While ZNS is similar to gabapentin and pregabalin, it confers greater protection than TPM as neuroprotective agent against inhibiting VGCC and NO activity, thereby alleviating neuropathy symptoms.

#### AUTHOR CONTRIBUTIONS

Investigation, methodology, writing original draft preparation—A.K.S.; Review and editing, conceptualization, supervision—C.D.U. All authors have read and agreed to the published version of the manuscript.

#### FINANCIAL SUPPORT

This work was supported by University Grant Commission (UGC) under Maulana Azad National Fellowship for Minority (F1-17.1/2012-13/MANF-2012-13-MUS-MAH-14758/ (SA-III/Website) dated 02/Jan 2012).

#### CONFLICT OF INTEREST

The authors declare no potential conflict of interest

#### ETHICAL APPROVALS

The Committee for the Purpose of Control and Supervision of Experiments on Animals, India. Prior approval was obtained from Shriman Sureshdada Jain College of Pharmacy's Institutional Animal Ethics Committee (2017/01) to conduct this research study.

#### DATA AVAILABILITY

All data generated and analyzed are included in this research article.

#### PUBLISHER'S NOTE

This journal remains neutral with regard to jurisdictional claims in published institutional affiliation.

#### REFERENCES

- Aebi H. Catalase *in vitro*. In: Methods in enzymology. Vol. 105. Elsevier, Amsterdam, The Netherlands, pp 121–6, 1984.
- Aurilio C, Pota V, Pace MC, Passavanti MB, Barbarisi M. Ionic channels and neuropathic pain: pathophysiology and applications. *J Cell Physiol*, 2008; 215(1):8–14.
- Baba M, Matsui N, Kuroha M, Wasaki Y, Ohwada S. Long-term safety and efficacy of mirogabalin in Asian patients with diabetic peripheral neuropathic pain. *J Diabetes Investig*, 2020; 11(3):693–8.
- Bektas N, Arslan, R, Ozturk Y. Zonisamide: antihyperalgesic efficacy, the role of serotonergic receptors on efficacy in a rat model for painful diabetic neuropathy. *Life Sci*, 2014; 95(1):9–13.
- Bennett GJ, Xie YK. A peripheral mononeuropathy in rat that produces disorders of pain sensation like those seen in man. *Pain*, 1988; 33(1):87–107.
- Bermejo PE, Anciones B. A review of the use of zonisamide in Parkinson's disease. *Ther Adv Neurol Disord*, 2009; 2(5):313–7.
- Bischofs S, Zelenka M, Sommer C. Evaluation of topiramate as an anti-hyperalgesic and neuroprotective agent in the peripheral nervous system. *J Peripher Nerv Syst*, 2004; 9(2):70–8.
- Biton V. Zonisamide: newer antiepileptic agent with multiple mechanisms of action. *Expert Rev Neurother*, 2004; 4(6):935–43.
- Bouhassira D. Neuropathic pain: definition, assessment and epidemiology. *Rev Neurol*, 2019; 175(1–2):16–25.
- Chaplan SR, Bach FW, Pogrel JW, Chung JM, Yaksh TL. Quantitative assessment of tactile allodynia in the rat paw. *J Neurosci Methods*, 1994; 53(1):55–63.
- Chen J, Li L, Chen SR, Chen H, Xie JD, Sirrieh RE, MacLean DM, Zhang Y, Zhou MH, Jayaraman V. Erratum: the  $\alpha$ 2 $\delta$ -1-NMDA receptor complex is critically involved in neuropathic pain development and gabapentin therapeutic actions. *Cell Rep*, 2022; 38(4):110308.
- Chen J, Liu X, Yu S, Liu J, Chen R, Zhang Y, Jiang L, Dai Q. A novel  $\omega$ -conotoxin Bu8 inhibiting N-type voltage-gated calcium channels displays potent analgesic activity. *Acta Pharm Sin B*, 2021a; 11(9):2685–93.
- Chen SM, Wang MH, Soung HS, Tseng HC, Fang CH, Lin YW, Yang CC, Tsai CC. Neuroprotective effect of L-theanine in a rat model of chronic constriction injury of sciatic nerve-induced neuropathic pain. *J Formos Med Assoc*, 2021b; 121(4):802–14.
- Chen J, Zhou X, Ding H, Zhan H, Yang F, Li W, Xie J, Liu X, Xu Y, Su M. Neuregulin-1-ErbB signaling promotes microglia activation contributing to mechanical allodynia of cyclophosphamide-induced cystitis. *NeuroUrol Urodyn*, 2019; 38(5):1250–60.
- Chong MS, Libretto SE. The rationale and use of topiramate for treating neuropathic pain. *Clin J Pain*, 2003; 19(1):59–68.
- Cui W, Wu H, Yu X, Song T, Xu X, Xu F. The calcium channel  $\alpha$ 2 $\delta$ 1 subunit: interactional targets in primary sensory neurons and role in neuropathic pain. *Front Cell Neurosci*, 2021; 15:397.
- Czeschik JC, Hagenacker T, Schäfers M, Büsselberg D. TNF- $\alpha$  differentially modulates ion channels of nociceptive neurons. *Neurosci Lett*, 2008; 434(3):293–8.
- Finnerup NB, Kuner R, Jensen TS. Neuropathic pain: from mechanisms to treatment. *Physiol Rev*, 2021; 101(1):259–301.
- Guevara I, Iwanejko J, Dembińska-Kieć A, Pankiewicz J, Wanat A, Anna P, Gołębek I, Bartuś S, Malczewska-Malec M, Szczudlik A. Determination of nitrite/nitrate in human biological material by the simple Griess reaction. *Clin Chim Acta*, 1998; 274(2):177–88.
- Hilaire C, Inquimbert P, Al-Jumaily M, Greuet D, Valmier J, Scamps F. Calcium dependence of axotomized sensory neurons excitability. *Neurosci Lett*, 2005; 380(3):330–4.

- Hjertén S, Pan H. Purification and characterization of two forms of a low-affinity Ca<sup>2+</sup>-ATPase from erythrocyte membranes. *Biochim Biophys Acta (BBA) Biomembr*, 1983; 728(2):281–8.
- Ilari S, Giancotti LA, Lauro F, Gliozzi M, Malafoglia V, Palma E, Tafani M, Russo MA, Tomino C, Fini M. Natural antioxidant control of neuropathic pain—exploring the role of mitochondrial sirt3 pathway. *Antioxidants*, 2020; 9(11):1103.
- Jibira Y, Boakye-Gyasi E, Kofi Mensah Abotsi W, Amponsah IK, Adongo DW, Woode E. Hydroethanolic stem bark extract of *Burkea africana* attenuates vincristine-induced peripheral neuropathy in rats. *Adv Pharmacol Pharm Sci*, 2020; 2020:7232579.
- Kandhare AD, Ghosh P, Ghule AE, Bodhankar SL. Elucidation of molecular mechanism involved in neuroprotective effect of C oenzyme Q 10 in alcohol-induced neuropathic pain. *Fundam Clin Pharmacol*, 2013; 27(6):603–22.
- Kang L, Tian Y, Xu S, Chen H. Oxaliplatin-induced peripheral neuropathy: clinical features, mechanisms, prevention and treatment. *J Neurol*, 2021; 268(9):3269–82.
- Kochi T, Nakamura Y, Ma S, Hisaoka-Nakashima K, Wang D, Liu K, Wake H, Nishibori M, Irifune M, Morioka N. Pretreatment with high mobility group box-1 monoclonal antibody prevents the onset of trigeminal neuropathy in mice with a distal infraorbital nerve chronic constriction injury. *Molecules*, 2021; 26(7):2035.
- Koshimizu H, Ohkawara B, Nakashima H, Ota K, Kanbara S, Inoue T, Tomita H, Sayo A, Kiryu-Seo S, Konishi H. Zonisamide ameliorates neuropathic pain partly by suppressing microglial activation in the spinal cord in a mouse model. *Life Sci*, 2020; 263:118577.
- Le Bars D, Adam F. Nociceptors and mediators in acute inflammatory pain. *Ann Fr Anesth Reanim*, 2002; 21(4):315–35.
- Lee JY, Choi HY, Park CS, Pyo MK, Yune TY, Kim GW, Chung SH. GS-KG9 ameliorates diabetic neuropathic pain induced by streptozotocin in rats. *J Ginseng Res*, 2019; 43(1):58–67.
- Lee J, Woo J, Favorov OV, Tommerdahl M, Lee CJ, Whitel BL. Columnar distribution of activity dependent gabaergic depolarization in sensorimotor cortical neurons. *Mol Brain*, 2012; 5(1):1–12.
- Levy D, Höke A, Zochodne DW. Local expression of inducible nitric oxide synthase in an animal model of neuropathic pain. *Neurosci Lett*, 1999; 260(3):207–9.
- Li J, Chen X, Lu X, Zhang C, Song Q, Feng L. Pregabalin treatment of peripheral nerve damage in a murine diabetic peripheral neuropathy model. *Acta Endocrinol (Bucharest)*, 2018; 14(3):294.
- Li K, Zhai M, Jiang L, Song F, Zhang B, Li J, Li H, Li B, Xia L, Xu L, Cao Y, He M, Zhu H, Zhang L, Liang H, Jin Z, Duan W, Wang S. Tetrahydrocurcumin ameliorates diabetic cardiomyopathy by attenuating high glucose-induced oxidative stress and fibrosis via activating the SIRT1 pathway. *Oxid Med Cell Longev*, 2019; 2019:6746907.
- Liu CH, Chang HM, Tseng TJ, Lan CT, Chen LY, Youn SC, Lee Jr J, Mai FD, Chou JF, Liao WC. Redistribution of Cav2. 1 channels and calcium ions in nerve terminals following end-to-side neurotaphy: ionic imaging analysis by TOF-SIMS. *Histochem Cell Biol*, 2016; 146(5):599–608.
- Liu QY, Chen W, Cui S, Liao FF, Yi M, Liu FY, Wan Y. Upregulation of Cav3. 2 T-type calcium channels in adjacent intact L4 dorsal root ganglion neurons in neuropathic pain rats with L5 spinal nerve ligation. *Neurosci Res*, 2019a; 142:30–7.
- Liu Q, Chen W, Fan X, Wang J, Fu S, Cui S, Liao F, Cai J, Wang X, Huang Y. Upregulation of interleukin-6 on Cav3. 2 T-type calcium channels in dorsal root ganglion neurons contributes to neuropathic pain in rats with spinal nerve ligation. *Exp Neurol*, 2019b; 317:226–43.
- Luo H, Liu HZ, Zhang WW, Matsuda M, Lv N, Chen G, Xu ZZ, Zhang YQ. Interleukin-17 regulates neuron-glia communications, synaptic transmission, and neuropathic pain after chemotherapy. *Cell Rep*, 2019; 29(8):2384–97.
- Malko P, Jiang LH. TRPM2 channel-mediated cell death: an important mechanism linking oxidative stress-inducing pathological factors to associated pathological conditions. *Redox Biol*, 2020; 37:101755.
- Mao M, Fan W, Zheng Y, Qi P, Xi M, Yao Y. Upregulation of N-Type voltage-gated calcium channels induces neuropathic pain in experimental autoimmune neuritis. *Evid Based Complement Altern Med*, 2022; 2022:8547095.
- Metwally MMM, Ebraheim LLM, Galal AAA. Potential therapeutic role of melatonin on STZ-induced diabetic central neuropathy: a biochemical, histopathological, immunohistochemical and ultrastructural study. *Acta Histochem*, 2018; 120(8):828–36.
- Micheli L, Rajagopalan R, Lucarini E, Toti A, Parisio C, Carrino D, Pacini A, Ghelardini C, Rajagopalan P, Di Cesare Mannelli L. Pain relieving and neuroprotective effects of non-opioid compound, DDD-028, in the rat model of paclitaxel-induced neuropathy. *Neurotherapeutics*, 2021; 18(3):2008–20.
- Misra HP, Fridovich I. The role of superoxide anion in the autoxidation of epinephrine and a simple assay for superoxide dismutase. *J Biol Chem*, 1972; 247(10):3170–5.
- Moron MS, Depierre JW, Mannervik B. Levels of glutathione, glutathione reductase and glutathione S-transferase activities in rat lung and liver. *Biochim Biophys Acta (BBA) Gen Subj*, 1979; 582(1):67–78.
- Murphy D, Lester D, Clay Smither F, Balakhanlou E. Peripheral neuropathic pain. *NeuroRehabilitation [Preprint]*, 2020:1–19.
- Murthy KNC, Vanitha A, Rajesha J, Swamy MM, Sowmya PR, Ravishankar GA. *In vivo* antioxidant activity of carotenoids from *Dunaliella salina*—a green microalga. *Life Sci*, 2005; 76(12):1381–90.
- Mutaraman A, Singh N. Attenuating effect of *Acorus calamus* extract in chronic constriction injury induced neuropathic pain in rats: an evidence of anti-oxidative, anti-inflammatory, neuroprotective and calcium inhibitory effects. *BMC Complement Altern Med*, 2011; 11(1):1–14.
- Naveed M, Ullah R, Khan A, Shal B, Khan AU, Khan SZ, Khan S. Anti-neuropathic pain activity of a cationic palladium (II) dithiocarbamate by suppressing the inflammatory mediators in paclitaxel-induced neuropathic pain model. *Mol Biol Rep*, 2021; 48(12):7647–56.
- Nazarbaghi S, Amiri-Nikpour MR, Eghbal AF, Valizadeh R. Comparison of the effect of topiramate versus gabapentin on neuropathic pain in patients with polyneuropathy: a randomized clinical trial. *Electron Physician*, 2017; 9(10):5617.
- Noh M, Stenkowski PL, Smith PA. Long-term actions of interleukin-1 $\beta$  on K<sup>+</sup>, Na<sup>+</sup> and Ca<sup>2+</sup> channel currents in small, IB4-positive dorsal root ganglion neurons: possible relevance to the etiology of neuropathic pain. *J Neuroimmunol*, 2019; 332:198–211.
- Palhares MR, Silva JF, Rezende MJS, Santos DC, Silva-Junior CA, Borges MH, Ferreira J, Gomez MV, Castro-Junior CJ. Synergistic antinociceptive effect of a calcium channel blocker and a TRPV1 blocker in an acute pain model in mice. *Life Sci*, 2017; 182:122–8.
- Pappagallo M. Newer antiepileptic drugs: possible uses in the treatment of neuropathic pain and migraine. *Clin Ther*, 2003; 25(10):2506–38.
- Paranos SL, Tomić MA, Micov AM, Stepanović-Petrović RM. The mechanisms of antihyperalgesic effect of topiramate in a rat model of inflammatory hyperalgesia. *Fundam Clin Pharmacol*, 2013; 27(3):319–28.
- Patel R, Dickenson AH. Mechanisms of the gabapentinoids and  $\alpha 2\delta$ -1 calcium channel subunit in neuropathic pain. *Pharmacol Res Perspect*, 2016; 4(2):e00205.
- Rajakulendran S, Hanna MG. The role of calcium channels in epilepsy. *Cold Spring Harb Perspect Med*, 2016; 6(1):a022723.
- Rosenberger DC, Blechschmidt V, Timmerman H, Wolff A, Treede RD. Challenges of neuropathic pain: focus on diabetic neuropathy. *J Neural Transm*, 2020; 127(4):589–624.
- Severenghaus JW, Ferree JW. Calcium determination by flame photometry; methods for serum, urine, and other fluids. *J Biol Chem*, 1950; 187:621–30.

Singh H, Kaur J, Arora R, Mannan R, Buttar HS, Arora S, Singh B. Ameliorative potential of *Argyrea speciosa* against CCI-induced neuropathic pain in rats: biochemical and histopathological studies. *J Ethnopharmacol*, 2020; 249:112399.

Slater TF, Sawyer BC. The stimulatory effects of carbon tetrachloride and other halogenoalkanes on peroxidative reactions in rat liver fractions *in vitro*. General features of the systems used. *Biochem J*, 1971; 123(5):805–14.

Stanzione F, Giangreco I, Cole JC. Use of molecular docking computational tools in drug discovery. *Prog Med Chem*, 2021; 60:273–343.

Teixeira-Santos L, Albino-Teixeira A, Pinho D. Neuroinflammation, oxidative stress and their interplay in neuropathic pain: focus on specialized pro-resolving mediators and NADPH oxidase inhibitors as potential therapeutic strategies. *Pharmacol Res*, 2020; 162:105280.

Verkhatsky A, Untiet V, Rose CR. Ionic signalling in astroglia beyond calcium. *J Physiol*, 2020; 598(9):1655–70.

Yang G, Wang Y, Yu Y, Zheng J, Chen J, Li S, Chen R, Zhang C, Naman CB, Yu D. Schekwanglupaside C, a new lupane saponin from *Schefflera kwangsiensis*, is a potent activator of sarcoplasmic reticulum Ca<sup>2+</sup>-ATPase. *Fitoterapia*, 2019; 137:104150.

Yang J, Xie MX, Hu L, Wang XF, Mai JZ, Li YY, Wu N, Zhang C, Li J, Pang RP. Upregulation of N-type calcium channels in the soma of uninjured dorsal root ganglion neurons contributes to neuropathic pain by increasing neuronal excitability following peripheral nerve injury. *Brain Behav Immun*, 2018; 71:52–65.

Yoon C, Wook YY, Sik NH, Ho KS, Mo CJ. Behavioral signs of ongoing pain and cold allodynia in a rat model of neuropathic pain. *Pain*, 1994; 59(3):369–76.

Zhang XM, Lun MH, Du W, Ma F, Huang ZQ. The  $\kappa$ -Opioid receptor agonist U50488H ameliorates neuropathic pain through the Ca<sup>2+</sup>/CaMKII/CREB pathway in rats. *J Inflamm Res*, 2022; 15:3039.

Zhou Y, Cai S, Gomez K, Wijeratne EM, Ji Y, Bellampalli SS, Luo S, Moutal A, Gunatilaka AA, Khanna R. 1-O-Acetylgeopyxin A, a derivative of a fungal metabolite, blocks tetrodotoxin-sensitive voltage-gated sodium, calcium channels and neuronal excitability which correlates with inhibition of neuropathic pain. *Mol Brain*, 2020; 13(1):1–12.

**How to cite this article:**

Upasani CD, Sherikar AK. Differential roles of blockade of Ca<sub>v</sub>2.2- $\alpha$ 2/ $\delta$ 1- $\beta$ 1 subtype calcium channel on two models of peripheral neuropathic pain. *J Appl Pharm Sci*, 2023. <http://doi.org/10.7324/JAPS.2023.137731>

Online First